

Defect Characterization for Scaling of QCA Devices

Jing Huang, Mariam Momenzadeh, Mehdi B. Tahoori and Fabrizio Lombardi
Dept of Electrical and Computer Engineering
Northeastern University
Boston, MA 02115
{ hjing,mmomenza,mtahoori,lombardi}@ece.neu.edu

Abstract

Quantum dot Cellular Automata (QCA) is amongst promising new computing scheme in the nano-scale regimes. As an emerging technology, QCA relies on radically different operations in its devices; for example, the logic values are represented by the position of electrons inside QCA cells rather than voltage levels, and the basic logic block of QCA is the majority voter. In this paper, we present the impact of scaling on defects that may arise in the manufacturing of QCA devices. This study shows how the sensitivity to manufacturing processing variations changes with device scaling. Scaling in QCA technology is related to cell dimension/size and cell-to-cell spacing within a Cartesian layout. Extensive simulation results on scaling of QCA devices, such as the majority voter, the inverter and the binary wire, are provided to show that defects have definitive trends in their behavior. These trends relate cell size (l) to the smallest cell-to-cell spacing (d) for erroneous behavior in the presence of different defects (such as misalignment and displacement); their impact on the correct functionality of QCA devices is extensively discussed. It is shown that in most defect cases the scaling relationship between l and d is linear, albeit with different slopes.

1 Introduction

Over the last few decades the exponential decrease in feature sizes and the substantial increase in processing power have been successfully achieved by conventional lithography based VLSI. However, serious challenges are encountered due to the approaching of the fundamental physical limits of CMOS technology (such as ultra-thin gate oxides, short channel effects, doping fluctuations) and increasingly difficult and expensive lithography at nano-scale. There has been extensive research in recent years at nano scale to supersede conventional CMOS by so-called emerging technologies (such as carbon tubes and tunneling devices); it is anticipated that these technologies can achieve a density of 10^{12} devices/ cm^2 and Tera Hertz frequencies with room temperature operation and ultra low power dissipation [8].

Among these new devices, *quantum dot cellular automata* (QCA) not only gives a solution at nano scale, but also it offers a new method of computation and information transformation [4]. The unique feature of QCA based designs is that logic states are not stored in voltage levels as in conventional electronics, but they are represented by the position of individual electrons. In terms of feature size, it is projected that a QCA cell of few nanometer size can be fabricated through molecular implementation by a self-assembly process.

The basic logic elements in this technology are the majority voter and the inverter. Binary wires and inverter chains are used as interconnect fabrics. In [12], QCA defects and related effects have been reported mostly at logic level. Testing of QCA devices and their unique features have

been investigated in [13]; [11] has considered the C-testability (where C stands for constant) of QCA designs based on majority voters. Based on these properties, test generation and design-for-testability techniques have been proposed [11]. While defective behavior of QCA is well understood with respect to kink energy among off-center cells, no work has been reported on the behavior of defects with respect to variations due to scaling in the physical features of QCA cells and devices.

In this paper, the impact of scaling QCA technology is investigated with respect to different defects (such as two-cell interaction and misplacement). Extensive simulation results on QCA devices of different cell sizes are reported which confirm the initial results in [12]. These results are used to characterize the effects of scaling by either cell dimension and/or cell spacing. This is important because for QCA, as a potential emerging technology, defects must be carefully considered in manufacturing to guide the choice in cell size and spacing. Such that desired tolerance to process variations can be achieved. The QCADesigner¹ v1.4.0 bistable engine is used in this paper to simulate various cell misplacement (displacement and misalignment) defects in basic QCA circuits. The simulation results suggest that in most cases a linear relationship between cell dimension and the smallest distance exists in the Cartesian plane to cause an erroneous behavior in a QCA device. However, the linear relationship has different slopes for the defects.

The rest of the paper is organized as follows. In Sec. 2, a brief review of QCA is presented. The defect model used in this work is described in Sec. 3. Simulation engine used as well as the scaling effects that are related to interaction between two cells are analyzed in Sec. 4. In Sec. 5, scaling is extended to basic QCA devices such as gates and the interconnect. Results are discussed and analyzed in Sec. 6, while conclusions are presented in Sec. 7.

2 QCA Review

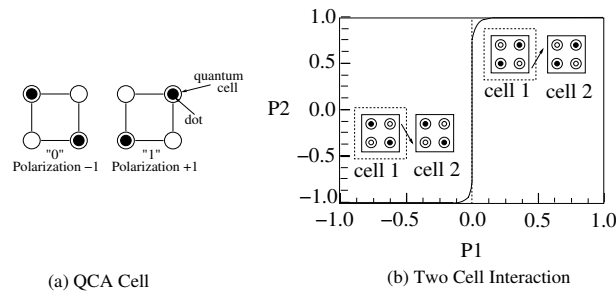


Figure 1. QCA cell and cell-to-cell response

A QCA cell can be viewed as a set of four charge containers or “dots”, positioned at the corners of a square. The cell contains two extra mobile electrons which can quantum mechanically tunnel between dots, but not cells. Coulomb repulsion forces the electrons to the corner positions, thus having the electrons aligned along either of the two diagonal axis. *Cell polarization level* is defined as the quantity which measures the extent to which the charge distribution is aligned along one of these axes [14]. Polarization $P = -1$ is used to represent logic “0” while Polarization $P = +1$ is logic “1”, as shown in Figure 1(a). Figure 1(b) illustrates the cell-to-cell response function, where the polarization P2 of cell 2 is induced by the fixed polarization of its neighbor cell 1 [14]. In the ground state of this two-cell system (which corresponds to correct computation), the polarization of cell 2 is aligned with its neighbor, the input cell 1. In an excited state, the cells align contrary to cell-to-cell electron repulsion and a *kink* is said to have occurred.

Unlike conventional logic in which information is transferred from one place to another by electrical current, QCA does so by the Coulomb interaction that connects the state of one cell to the

¹QCADesigner is developed by ATIPS lab in University of Calgary in Canada

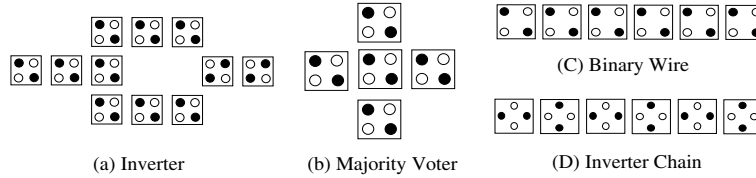


Figure 2. Basic QCA devices

state of its neighbors. This results in a technology in which information transfer (interconnection) is the same as information transformation (logic manipulation). Power dissipation in QCA circuits is ultra low compared with conventional CMOS circuits [14].

The basic logic gate in QCA is the *majority voter*. The majority voter with logic function $MV(A, B, C) = AB + AC + BC$, can be realized by only 5 QCA cells (compared to a CMOS implementation which requires 16 transistors), as shown in Figure 2(b). Logic AND and logic OR functions can be implemented from the majority voter by setting an input (the programming input) permanently to a 0 or 1 value. The inverter is shown in Figure 2(a). The binary wire and inverter chain (as interconnect fabric) are shown in Figure 2(c)(d).

The concept of clocking for QCAs has been introduced in [5]. Some high level designs including the RAM and microprocessors have been proposed [7][10]. Currently, micro-sized QCA devices have been fabricated with metal cells which operates at 50mk [3][4]. Sequential circuits have also been fabricated using metal tunnel junction technology; the operation of a QCA latch and a two-bit shift register have been demonstrated in [6]. Recent research has focused on fabricating molecular-sized QCA, in which higher speed and room-temperature operation can be realistically expected. [9] has proposed few possible molecular realizations and advances for surface attachment chemistry compatible with QCA.

3 Defect Model

To perform a defect characterization of QCA devices and circuits and study their effects at logic-level, appropriate defect mechanisms and models have been proposed [13]. According to [1], in the present stage of QCA manufacturing, defects are possible in both the *synthesis* phase (where the individual cells are manufactured) and the *deposition* phase (where the cells are attached to a surface). Manufacturing defects may cause a cell to have missing or extra dots or/and electrons. These defects are fatal and easy to detect; a missing (or additional) dot is very unlikely due to the ease of purification of small inorganic molecules [1]. Defects are much more likely to occur in the deposition phase than in the synthesis phase due to its inherent difficulty, thus resulting in misplacement while placing individual cells in specific locations. Various types of cell misplacement defects may occur such as misalignment, displacement, rotation, etc. Therefore in this paper, only cell defects in the deposition phase are considered. The effects of the following types of cell misplacement are analyzed:

- A *cell displacement* is a defect in which the defective cell is misplaced from its original direction.
- In a *cell misalignment* defect, the direction of the defective cell is not properly aligned.

At manufacturing, noise due to thermal effects (commonly resulting in kinks) is not present and therefore they are not considered (during operation, kinks can be avoided by adjusting the timing and clocking features of the QCA circuit as well as its operating temperature [8]). While these defects were considered in our previous work [13] [12], the objective of this paper is to assess whether scaling of QCA will have an impact on the correct operation of cells as well as more complex devices (such as the majority voter and the inverter). It is well known that for kink (as a change in polarity) to occur, the defining rule for the energy follows a relationship in $r^{-5}\cos(4\phi)$, where r is the distance between the centers of a (correctly placed) cell and an off-center (misplaced) cell and ϕ is the angle

of misplacement, i.e. as the distance between two cells is increased, the kink energy decreases and effectively a smaller amount of external energy could excite a cell into an erroneous (polarization) state. Such relationship however is not known for defects which involve multiple cells (arranged in a Cartesian layout for some basic QCA devices such as the majority voter and the inverter). Moreover it is assumed that all devices are within one clocking zone.

4 Cell Scaling

QCADesigner v1.4.0 [2] for UNIX, which is developed by ATIPS lab in the University of Calgary, is used in this work. Our results are obtained using the *Bistable Engine* [2]. In the bistable engine, each cell is modeled as a simple two-state system. The bistable engine utilizes an approximation based on the interaction between cells, namely the interaction strength between two cells decays inversely with the fifth power of the distance separating them. Hence only those effects within an area specified by a radius R , are considered for each cell. For cell i , its two-state system model is mathematically described by the following Hamiltonian:

$$H_i = \sum_j \begin{bmatrix} -\frac{1}{2}P_j E_{i,j}^k & -\gamma \\ -\gamma & \frac{1}{2}P_j E_{i,j}^k \end{bmatrix} \quad (1)$$

$E_{i,j}^k$ is the kink energy between the two cells (i and j), which represents the energy cost of opposite polarization in the two cells; P_j is the polarization of cell j ; γ is the tunneling energy between two dots in a cell. For each cell i , the sum of the Hamiltonian is over all cells (i.e. j) within its *radius of effect* R . Switching is assumed to be adiabatic, i.e. the system remains very close to the energy ground state during transition. Therefore, the stationary state of each cell can be obtained by solving the time-independent Schroedinger equation. The QCADesigner engine uses the Jacobi algorithm to find the eigenvalues and eigenvectors of the Hamiltonian. The engine computes the polarization of each cell until the whole system converges.

In this paper, the radius of effect R used in the simulation has been set to four times the cell size (as commonly found in practice for metal QCA). The number of samples is set to 6400. All other parameters are set to their default value.

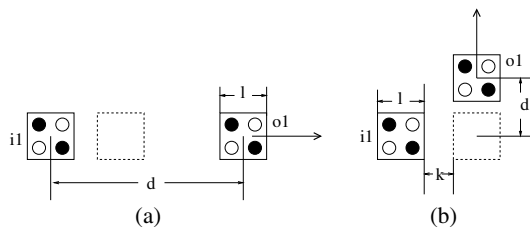


Figure 3. Scaling among two cells

The basic functionality of QCA is based on the Coulombic interaction among neighboring cells; this depends on the distance as well as the angle between the two cells. In this section, the simplest case of two cell interaction is studied through simulation by scaling the cell size. Each cell is assumed to have a size given by $l \times l$ (all dimensions in nanometers, nm). The radius of effect is $R = 4 \times l$. Consider initially a horizontal displacement (as shown in Figure 3(a)) in which two cells (one input and one output) are aligned. In this case, scaling is related to cell size and the distance by which two cells can interact for correct polarity. By increasing the horizontal center-to-center distance, polarization can be lost. The smallest of such distance is denoted by d . The simulation results for cell dimension l versus d for horizontal displacement are plotted in Figure 4. As expected, the smallest center-to-center distance such that the two cells have no interaction is defined by the *radius of effect* R , which is a parameter in the bistable engine. The output cell is fully polarized whenever the distance is smaller than R , no gradual polarization level drop can be observed with this engine.

Next consider the vertical misalignment as depicted in Figure 3(b). The cells are again of size $l \times l$, placed k nanometers apart. In the defect free case, the output cell has the same polarization as the input cell. Consider a misalignment defect in which the output cell is moved in the vertical direction. The smallest vertical distance to cause an erroneous output is again denoted by d . l and k are scaled in the same proportion and the results are plotted as d versus l in Figure 4. In this case, the simulation results show that any misalignment greater or equal to half of the cell size causes an incorrect output; this is in agreement with our previous results as reported in [12]. This correctly confirms that a half cell shift in the vertical direction creates an inversion in QCA.

Note that the two diagrams in Figure 4 have different Y-axis ranges. The slope for horizontal displacement is approximately ten times more than that of the vertical misalignment. This suggests that QCA is much more sensitive towards vertical misalignment than horizontal displacement.

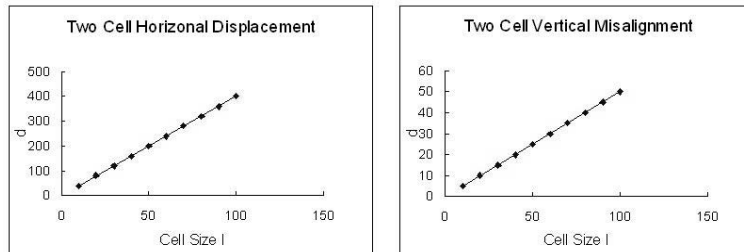


Figure 4. Simulation results for two cell interaction

5 Device Scaling

In this section, the scaling effects of defects on few QCA devices (as basic building blocks of this technology) are provided. The following devices are considered: the majority voter, the inverter and the binary wire. As before, the dimension of a square cell is denoted by l ; in all cases of scaling in the cell dimension, the cell-to-cell distance k is scaled by the same factor (constant scaling), i.e. the ratio of l and k is constant. R is again set to equal four times the cell size.

5.1 Double Binary Wire

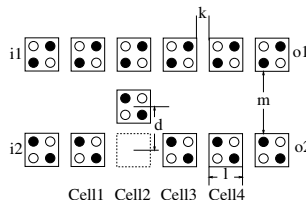


Figure 5. Double binary wire bridging defects

Consider the binary wire which is commonly used as interconnect for QCA circuits. The two parallel binary wires are placed m nanometers apart as shown in Figure 5. The cells in the same wire have a horizontal distance of k nanometers. m is chosen to be sufficiently large such that in the defect free case, the wires do not interfere with each other, i.e. $o1 = i1$ and $o2 = i2$. For a cell size of l , the values of $k = \frac{1}{2}l$ and $m = 3l$ were chosen. A bridging may occur by moving at least one cell of the bottom wire upwards, as shown in Figure 5. The smallest distance which causes a defective output is denoted by d . The above process is repeated under different cell sizes; simulation results are shown in Figure 6. Three bridging defects are considered: (1)moving cell 2 up; (2)moving cell 4 up; (3)moving cell 1, cell 3 up. The defect resulting from moving cell 2 upward is illustrated in

Figure 5. Additionally, the best fitting linear lines are also shown. The results for moving cell 4 upward is exactly the same as those of moving cell 2 upward. Similar results are observed for all three cases of bridging defects. As reported in [13], wire bridging faults discussed here cause the bottom wire to be the victim of the upper wire, i.e. the output of the bottom wire is controlled by the input of the upper wire. Clearly, the normalized defect tolerance d/l (normalized to cell size) is constant with respect to cell size, which means that the sensitivity to manufacturing process variations remains almost unchanged in scaling.

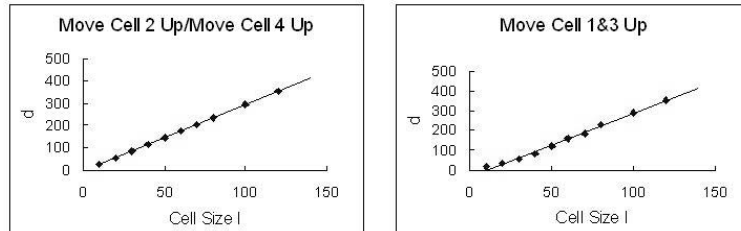


Figure 6. Scaling for double binary wire bridging defects

5.2 Majority Voter

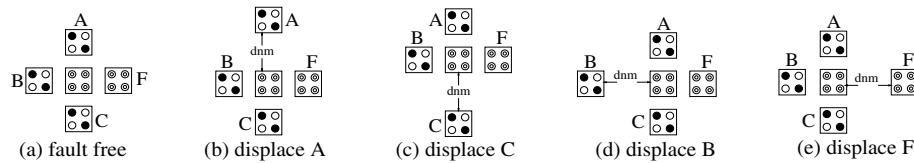


Figure 7. Displacement defects in majority voter

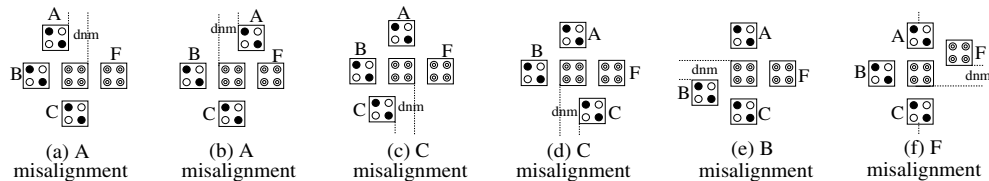


Figure 8. Misalignment defects in majority voter

The Majority Voter (MV) is the basic logic element in QCA; it can be programmed to realize both AND and OR functions by fixing one of its inputs. The detailed defect characterization of MV has been reported in [12]; testing as well as design-for-testability considerations for MV based circuits can be found in [11]. In this section, scaling is simulated such that various MV displacement and misalignment defects are considered, as shown in Figure 7 and 8. The smallest distance which a cell is moved to generate an erroneous output is denoted by d . Scaling for MV defects has been simulated and the results are shown in Figure 9 and 10. Linear fitting lines are shown in these figures. As in previous cases, almost all defect trends are linear with respect to the cell size. This indicates that for many types of MV misplacement (including displacement and misalignment) defects, the normalized tolerance d/l remains almost unchanged with device scaling.

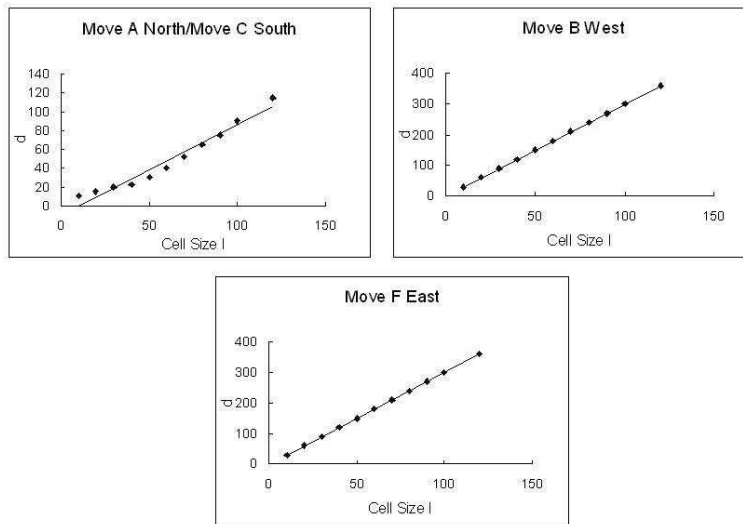


Figure 9. Scaling for displacement defects in MV

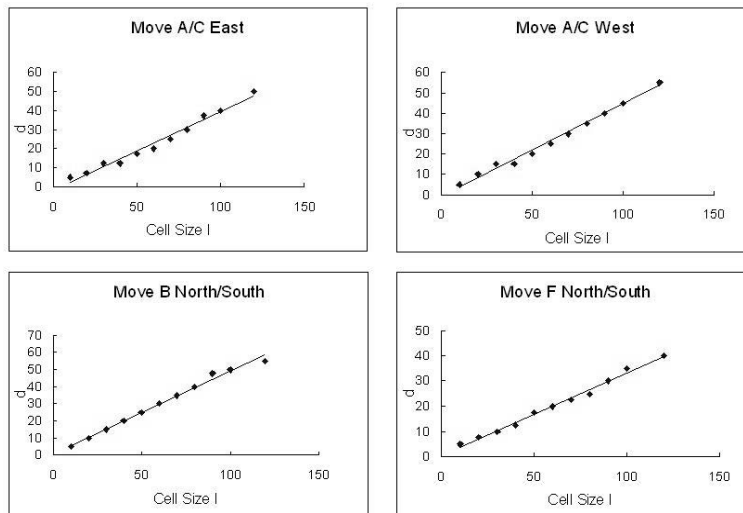


Figure 10. Scaling for misalignment defects in MV

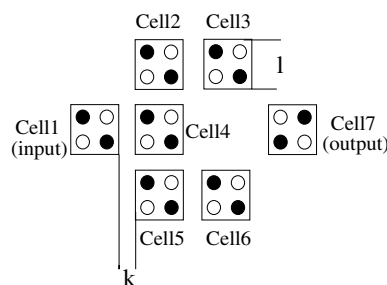


Figure 11. QCA inverter

5.3 Inverter

The inverter is considered next. In QCA, inversion can be realized in different ways, such as the inverter shown in Figure 2 or by simply shifting a cell by half cell size in a 45 degrees orientation. The inverter consisting of 7 cells is considered in this paper (Figure 11); this device is more robust than the inverter created by the half cell size shift, yet it is still reasonably small. In the defect free case, the cell-to-cell distance is given by k nanometers such that $k = \frac{1}{4}l$ where l is the cell size. Two cell misalignment defects have been simulated: moving cell 1 (the input cell) north (i.e. upward) and moving cell 7 (output) north. Results are plotted in Figure 12. Similar to the results for MV and binary wires, the misalignment defect tolerance for the output cell (cell 7) is linear with respect to cell size. However, the misalignment defect for the input cell (cell 1) behaves quite differently. As the cell size increases, at first the defect tolerance increases; then at $l = 60$ it levels off, then start to decrease at $l = 120$. By using the QCADesigner v1.4.0 bistable engine, the inverter with $l = 140$ ceases its functionality, i.e. it behaves as a wire with equal input and output. Additionally, the best fitting polynomial line (of highest degree of 6) is also shown.

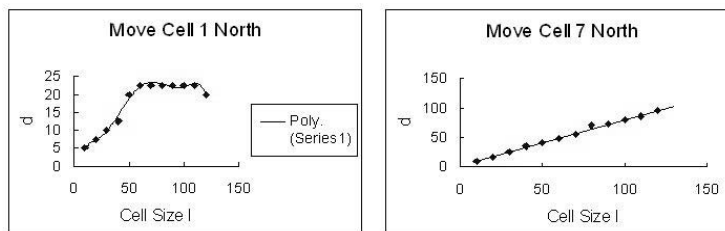


Figure 12. Scaling for displacement defects in a QCA inverter

6 Discussion

Previous sections have presented simulation results for scaling by considering the size of a QCA cell versus the smallest distance causing an erroneous behavior due to different defects (such as misalignment or displacement). Note that in all experiments, the inter-cell distance is limited by the resolution in the user interface of the simulation tool; in QCA Designer v1.4.0, the grid size is set to 2.5 nanometers. The following conclusions can be drawn from the simulation results.

- For the two-cell case, scaling (under the constant ratio of l and k or constant scaling) seems to have a linear relationship on both displacement and misalignment defects. This is consistent with results reported in other papers [12] [13], confirming that the loss of polarity once two cells are separated by at least half of cell size (in the case of a misalignment defect in the vertical direction). Additionally, from Figure 4 it can be seen that the slope for horizontal displacement is approximately ten times larger than that for the vertical misalignment. This suggests that the vertical direction is more sensitive to process variations compared to the horizontal direction.
- For all cases of defects affecting the double parallel wires in QCA, the relationship between d and l follows a linear relationship. In other words, the normalized defect tolerance d/l is constant in scaling. Therefore, the sensitivity to process variation scales in the same proportion to device scaling.
- For the Majority Voter (MV), all simulated misalignment defects result in an increase in d which is almost linear with respect to cell size. Its defect tolerance is equal or slightly less than half cell size, which confirms our results in [13], i.e. an half cell misalignment creates an unwanted inverting effect, thus causing the gate to malfunction. The simulation results for the displacement of the horizontal input B show again a linear relationship. In this case $d=R$

for all cell sizes, so the tolerance of the displacement of input B in our simulation is limited by the radius of effect in the simulation engine. For the side input cells (i.e. A and C), clearly the defect tolerance is smaller than for B , and some nonlinear behavior is present. This confirms previous studies [13] that in an MV B is the dominant cell.

- For the 7-cell inverter, a clearly nonlinear relationship is observed in the misalignment defect of the input cell. Simulation results show that maximum defect tolerance occurs for cell size between $70nm$ and $110nm$, i.e. by further increasing the cell size a decrease in fault tolerance occurs. This implies that tolerance to this defect must be carefully assessed in the manufacturing process.

7 Conclusion

Quantum dot Cellular Automata (QCA) is an emerging technology which is promising for nano scale implementation. In this paper, scaling has been extensively analyzed to establish the tolerance to different defects once the cell dimension and cell-to-cell spacing are changed. This work investigates how the sensitivity to manufacturing process variations scales with device scaling. In particular the effects of defects due to misalignment and displacement in different QCA devices (such as the majority voter, the double wire and the inverter) have established that in most cases the relationship between cell dimension and the smallest distance for erroneous behavior is linear. This is a novel characterization that can be used to assess the viability of QCA as a technology in the nano ranges.

References

- [1] Personal communication with Professor Marya Lieberman, Department of Chemistry and Biochemistry, University of Notre Dame, IN, USA.
- [2] QCADesigner Home Page : www.qcadesigner.ca.
- [3] A.O.Orlov, I.Amlani, G.H.Bernstein, C.S.Lent, and G.L.Snider. Realization of a Functional Cell for Quantum-Dot Cellular Automata . In *Science*, volume 277, pages 928–930, 1997.
- [4] I.Amlani, A.O.Orlov, G.L.Snider, and C.S.Lent. Demonstration of a Six-dot Quantum Cellular Automata System . In *Applied Physics Letters*, volume 72, pages 2179–2181, 1998.
- [5] K.Hennessy and C.S.Lent. Clocking of Molecular Quantum-Dot Cellular Automata . In *Journal of Vacuum Science and Technology*, volume 19(5), pages 1752–1755, 2001.
- [6] R.K. Kummamuru, A.O. Orlov, C.S. Lent, G.H. Bernstein, and G.L. Snider. Clocked Quantum-Dot Cellular Automata Circuits. In *NanoTechnology Conference and Tradeshow*, volume 2, pages 149–152, 2003.
- [7] K.Walus, A.Vetteth, G.A.Jullien, and V.S.Dimitrov. RAM Design Using Quantum-Dot Cellular Automata . In *NanoTechnology Conference and Trade Show*, volume 2, pages 160–163, 2003.
- [8] C.S. Lent and B. Lsaksen. Clocked Molecular Quantum-Dot Cellular Automata. In *IEEE Transactions on Electron Devices*, volume 50, 2003.
- [9] M. Lieberman, S. Chellamma, B. Varughese, Y. Wang, C.S. Lent, G.H. Bernstein, G. Snider, and F.Peiris. Quantum-Dot Cellular Automata at a Molecular Scale . In *Annals of the New York Academy of Sciences*, volume 960, pages 225–239, 2002.
- [10] M.T. Niemier and P.M.Kogge. Logic-in-Wire: Using Quantum Dots to Implement a Microprocessor . In *International Conference on Electronics, Circuits, and Systems*, 1999.
- [11] M.B. Tahoori, J. Huang, M. Momenzadeh, and F. Lombardi. Testing of Quantum Cellular Automata . In *Accepted by IEEE Transaction on Nanotechnology*, 2004.
- [12] M.B. Tahoori, M. Momenzadeh, J. Huang, and F. Lombardi. Defect and Fault Characterization in Quantum Cellular Automata . In *NanoTechnology Conference and Trade Show*, 2004.
- [13] M.B. Tahoori, M. Momenzadeh, J. Huang, and F. Lombardi. Defects and Faults in Quantum Cellular Automata at Nano Scale . In *VLSI Test Symposium (VTS)*, pages 291–296, 2004.
- [14] P.D. Tougaw and C.S. Lent. Logical Devices Implemented Using Quantum Cellular Automata . In *Journal of Applied Physics*, volume 75(3), pages 1818–1825, 1994.